

High Temperature, High Power InGaAs/GaAs Quantum-Well Lasers with Lattice-Matched InGaP Cladding Layers

M. C. Wu, Y. K. Chen, J. M. Kuo, M. A. Chin, and A. M. Sergent

Abstract—We report the high temperature and high power operation of the strained-layer InGaAs/GaAs quantum well lasers with lattice-matched InGaP cladding layers grown by gas-source molecular beam epitaxy. Self-aligned ridge waveguide lasers of 3 μm width were fabricated. These lasers have low threshold currents (7 mA for 250- μm -long cavity and 12 mA for 500- μm -long cavity), high external quantum efficiencies (0.9 mW/mA), and high peak powers (160 mW for 3- μm -wide laser and 285 mW for 5- μm -wide laser) at room temperature under continuous wave (CW) conditions. The CW operating temperature of 185°C is the highest ever reported for the InGaAs/GaAs/InGaP quantum well lasers, and is comparable to the best result (200°C) reported for the InGaAs/GaAs/AlGaAs lasers.

HIGH power strained-layer InGaAs semiconductor quantum-well lasers are of great interest for their applications in optical data storage, free-space optical interconnects, pumping of solid-state lasers, and more recently, pumping of erbium-doped fiber amplifiers (EDFA) at 980 nm wavelength [1], [2]. Most of these applications require high output power, wide ranges of operation temperature and long-term reliability. Conventionally, the InGaAs quantum well lasers are grown on GaAs substrates using AlGaAs cladding layers. Good laser performance has been obtained [3]. However, previous studies show that facet oxidation causes laser degradation and affects its long term reliability [4]. This problem can be alleviated by using an aluminum-free $\text{In}_{0.49}\text{Ga}_{0.51}\text{P}$ cladding layer, which has a much slower oxidation rate. Very low recombination velocity (1.5 cm/s) at the InGaP/GaAs heterointerfaces has also been reported [5]. The use of InGaP cladding layers have been demonstrated in semiconductor lasers with lattice-matched active media [6]–[8]. The aluminum-free feature also greatly simplifies the epitaxial regrowth process required for more sophisticated laser structures. Furthermore, wet chemical etchants with great selectivities between InGaP and GaAs are readily available. All these features have enabled us to make high performance lasers with the InGaP/GaAs materials system.

The $\text{In}_{0.49}\text{Ga}_{0.51}\text{P}$ is lattice matched to GaAs, and has a bandgap energy of 1.91 eV (\sim that of $\text{Al}_{0.4}\text{Ga}_{0.6}\text{As}$). The

InGaAs/GaAs single quantum well lasers with InGaP cladding layers grown by metalorganic chemical vapor deposition (MOCVD) were previously reported [9]. Mass-transported InGaAs strained-quantum-well lasers were also fabricated [10]. However, the high temperature performance of these layers have not been explored. In contrast to the GaAs/AlGaAs heterostructures, most of the energy bandgap difference of GaAs/InGaP lies in the valence band. The heterobarriers for confining electrons in the active region is much smaller than those in GaAs/AlGaAs. For example, the conduction band discontinuity ΔE_C between $\text{In}_{0.49}\text{Ga}_{0.51}\text{P}$ and GaAs is 108 meV [11], [12], as compared to 299 meV between $\text{Al}_{0.4}\text{Ga}_{0.6}\text{As}$ and GaAs [13]. Because the electrons have small effective mass, it is very important to investigate the efficiency of the electron confinement, especially at high temperatures and under high current injection (high power) conditions. In this letter, we report on the high temperature and high power performance of the first InGaAs/GaAs/InGaP quantum-well laser grown by gas-source molecular beam epitaxy (GSMBE). The 3 μm -wide self-aligned ridge waveguide laser has a threshold current of 12 mA, a peak power of 160 mW (285 mW for 5 μm -wide devices), and operates in continuous wave (CW) up to 185°C. This performance is comparable to the best reported InGaAs/GaAs lasers with conventional AlGaAs cladding layers.

The schematic diagram of the device structure is shown in Fig. 1. A separate confinement heterostructure (SCH) is used here to provide confinement of electrical carriers as well as optical field. The epitaxial layers are grown by GSMBE. The active region consists of three 70 Å-thick $\text{In}_{0.2}\text{Ga}_{0.8}\text{As}$ quantum wells and two 200 Å-thick GaAs barriers. The active region is sandwiched between two 1000 Å-thick GaAs separate confinement layers. The active and the SCH region are cladded by $\text{In}_{0.49}\text{Ga}_{0.51}\text{P}$, which is lattice matched to GaAs to within 5×10^{-4} . An n^+ GaAs layer and a GaAs/InGaP superlattice buffer are grown before the lower cladding layer to improve the crystal quality. The laser thus grown has a threshold current density of 177 A/cm² for 500 μm -long cavities. The detailed growth procedure and the broad-area laser characteristics have been reported elsewhere [14].

To facilitate the fabrication of ridge waveguide lasers, a thin GaAs stop-etch layer is inserted in the upper InGaP cladding layer. Ridge waveguides of 3 μm width are

Manuscript received March 9, 1992; revised April 29, 1992.
The authors are with AT&T Bell Laboratories, Murray Hill, NJ 07974.

IEEE Log Number 9201655.

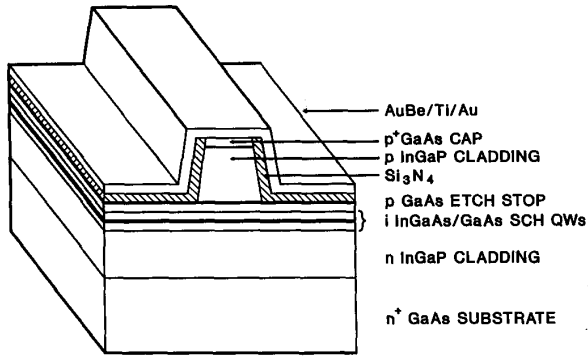


Fig. 1. The schematic of the self-aligned ridge-waveguide InGaAs/GaAs quantum-well laser with lattice-matched InGaP cladding layers.

formed by selective wet chemical etching, which removes the InGaP material above the stop-etch layer. Then the etched wafer is covered by Si₃N₄ and a self-aligned process [15] is used to define the p-contact opening on top of the ridge. Standard metalization and cleaving processes are used to finish the fabrication. The laser is mounted p-side up for testing. The ridge waveguide lasers have very low threshold currents: 7 mA for 250- μ m-long cavities and 12 mA for 500- μ m-long cavities at room temperature under CW conditions, as shown in Fig. 2. External differential quantum efficiency as high as 0.9 mW/mA is obtained for 250- μ m-long lasers. From the slope of inverse quantum efficiency versus cavity length, a very low internal waveguide loss of 7 cm⁻¹ is obtained. The emission wavelength is 1.02 μ m.

A 500 μ m-long laser was anti-reflection/high-reflection (AR/HR) coated for evaluating its high temperature performance. Fig. 3 shows the CW light-versus-current (*L-I*) curves for temperatures from 30°C to 185°C. Despite the much smaller heterobarrier for electron confinement, the highest CW operating temperature of 185°C is comparable to the best performance reported (200°C) for the InGaAs/GaAs laser with Al_{0.60}Ga_{0.4}As cladding layers [16]. Fig. 4 shows the variation of the CW threshold current with temperature. A characteristic temperature of $T_0 = 180$ K is obtained between 30°C and 60°C. The T_0 is cavity-length dependent: $T_0 = 185$ K for 750- μ m-long lasers, $T_0 = 180$ K for 500- μ m-long lasers, and $T_0 = 135$ K for 250- μ m-long lasers. The cavity length also affects the maximum operable temperature. For cavity lengths < 500 μ m, longer lasers have higher maximum operable temperatures because of the larger T_0 . However, the maximum operable temperature drops for cavity length > 500 μ m because the increase of T_0 have saturated while the absolute threshold currents continue to increase.

The T_0 is smaller for shorter lasers because the gain of the quantum wells saturates very rapidly with the carriers concentrations. Shorter lasers have higher threshold gain and, therefore, higher carrier concentrations at threshold.

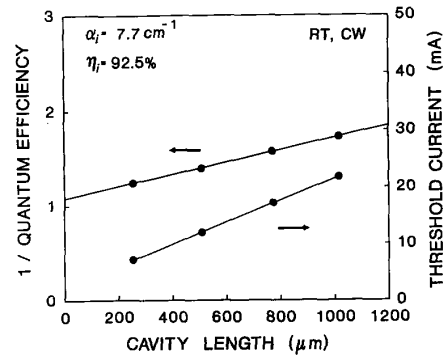


Fig. 2. The inverse external differential quantum efficiency and the threshold current versus the cavity length. The extrapolated internal quantum efficiency is 92.5% and the internal waveguide loss is 7.7 cm⁻¹.

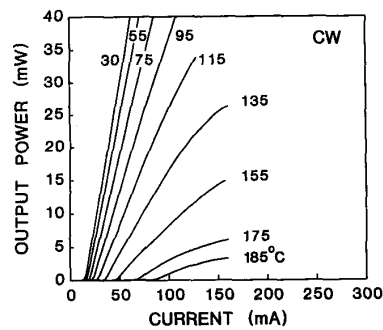


Fig. 3. The CW light-versus-current characteristics of an AR/HR coated InGaAs/GaAs/InGaP quantum well laser (3 μ m \times 500 μ m) for temperatures from 30°C to 185°C.

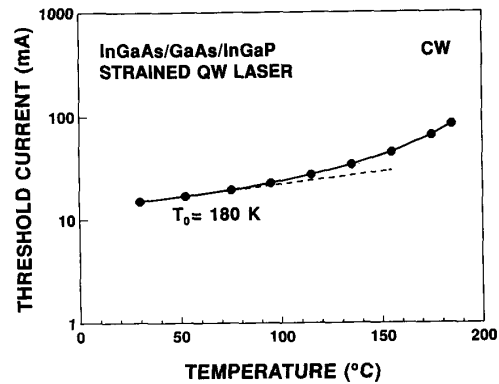


Fig. 4. The CW threshold current versus the heat sink temperature. The characteristic temperature, T_0 , is 180 K between 30°C and 60°C.

Low injection level at threshold is very important to achieve high T_0 . The use of multiple quantum-well active region also helps the high temperature operation because it reduces the threshold gain *per quantum well* and, therefore, decreases threshold carrier concentrations in each

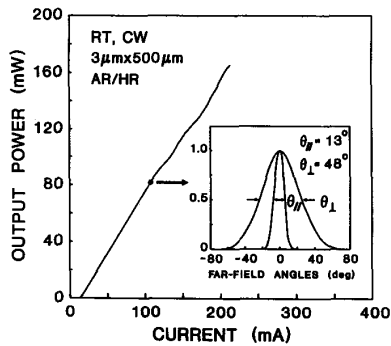


Fig. 5. The CW light-versus-current curve of a $3 \mu\text{m} \times 500 \mu\text{m}$ AR/HR coated InGaAs/GaAs/InGaP laser at room temperature. The peak output power is 160 mW. The inset shows the far-field patterns of the laser at 80 mW.

well. This is consistent with the previously reported results of the InGaAs/GaAs/InGaP single quantum well laser ($T_0 = 130 \text{ K}$ [9]), and the InGaAs/AlGaAs single quantum well laser ($T_0 = 140 \text{ K}$ [16]). With tighter optical confinement as well as electrical carrier confinement, lasers with $T_0 > 200 \text{ K}$ have been reported for some InGaAs/AlGaAs [15] and GaAs/AlGaAs [17] multiple quantum well lasers and bulk double heterostructure lasers [18].

The high power performance is illustrated in Fig. 5. The laser is $3 \mu\text{m}$ wide and $500 \mu\text{m}$ long, and is AR/HR coated. The reflectivities of the AR- and HR-coated facets are approximately 5% and 90%, respectively. A peak power of 160 mW is obtained before reaching catastrophic optical damage (COD). Higher peak power at 285 mW is obtained for lasers with slightly wider ridge width of $5 \mu\text{m}$. The far-field patterns measured at 80 mW are shown in the inset of Fig. 5. The lateral and transverse far-field angles (full-width-half-maximum) are $\theta_{||} = 13^\circ$ and $\theta_{\perp} = 48^\circ$, respectively. The aspect ratio is $\theta_{\perp}/\theta_{||} = 3.7:1$. Circular beam divergence can be achieved by using a periodic-index separate confinement heterostructure (PINSCH) [19], which has the advantage of reducing the vertical beam divergence without employing any other intermediate lattice-matched InGaAsP quaternary layers in the GaAs/InGaP materials system. The laser operates in a single lateral mode up to 90 mW of output power. High order lateral modes start to appear at higher power. Though they can be suppressed by optimizing the ridge waveguide structure, a more attractive alternative is to use strong index-guided structures such as buried heterostructure (BH). Multiple-step epitaxial growth needed for BH is easily accomplished in the InGaAs/GaAs/InGaP materials system because the material is free of aluminum, which is notorious for difficult regrowth process. Recently, we have also demonstrated a self-aligned InGaAs/GaAs/InGaP quantum well lasers with two GSMBE growth steps [20]. Another BH utilizing the mass transport property of InGaP has also been demonstrated [8], [10].

In conclusion, the high temperature and high power

operation of the InGaAs/GaAs/InGaP quantum well laser grown by gas-source molecular beam epitaxy is demonstrated for the first time. The ridge waveguide laser ($3 \mu\text{m} \times 500 \mu\text{m}$) has a threshold current of 12 mA, an external differential quantum efficiency of 0.9 mW/mA, a characteristic temperature T_0 of 180 K, and a peak power of 160 mW. The CW operating temperature of 185°C is the highest ever reported in this materials system and is comparable to the best performance reported for the InGaAs/GaAs/AlGaAs materials system.

REFERENCES

- [1] M. Yamada, M. Shimizu, T. Takeshita, M. Okayasu, N. Horiguchi, S. Uehara, and E. Sugita, "Er³⁺-doped fiber optical amplifier pumped by 0.98 μm laser diodes," *IEEE Photon. Technol. Lett.*, vol. 1, pp. 422-424, 1989.
- [2] M. C. Wu, N. A. Olsson, D. Sivco, and A. Y. Cho, "A 970 nm strained-layer InGaAs/GaAlAs quantum well laser for pumping an erbium-doped optical fiber amplifier," *Appl. Phys. Lett.*, vol. 56, pp. 221-223, 1990.
- [3] H. K. Choi and C. A. Wang, "InGaAs/AlGaAs strained single quantum well diode lasers with extremely low threshold current density and high efficiency," *Appl. Phys. Lett.*, vol. 47, pp. 321-323, 1990.
- [4] T. Yuasa, M. Ogawa, K. Endo, and H. Yonezu, "Degradation of (AlGa)As DH lasers due to facet oxidation," *Appl. Phys. Lett.*, vol. 32, pp. 119-121, 1978.
- [5] J. M. Olson, R. K. Ahrenkiel, D. J. Dunlavy, B. Keyes, and A. E. Kibbler, "Ultralow recombination velocity at Ga_{0.5}In_{0.5}P/GaAs heterostructures," *Appl. Phys. Lett.*, vol. 55, pp. 1208-1210, 1989.
- [6] C. J. Nuese, G. H. Olsen, and M. Ettenberg, "Vapor-grown cw room-temperature GaAs/In_yGa_{1-y}P lasers," *Appl. Phys. Lett.*, vol. 29, pp. 54-56, 1976.
- [7] Zh. I. Alferov, N. Yu. Antonishkis, I. N. Arsent'ev, D. Z. Garbuzov, V. I. Kolyshkin, T. A. Nalet, N. A. Strugov, and A. V. Tikunov, "Quantum-well separate-confinement InGaAsP/GaAs ($\lambda = 0.86-0.78 \mu\text{m}$) laser ($J_{th} = 100 \text{ A/cm}^2$, efficiency 59%)," *Sov. Tech. Phys.*, vol. 22, pp. 650-652, 1988.
- [8] S. H. Groves, Z. L. Liao, S. C. Palmateer, and J. N. Walpole, "GaInP mass transport and GaInP/GaAs buried heterostructure lasers," *Appl. Phys. Lett.*, vol. 56, pp. 312-314, 1990.
- [9] T. Ijichi, M. Ohkubo, N. Matsumoto, and H. Okamoto, "High Power CW operation of aluminum-free InGaAs/GaAs/InGaP strained layer single quantum well ridge waveguide lasers," presented at 12th Internat. Semiconductor Laser Conf., paper D-2, Sept. 1990, Davos, Switzerland.
- [10] Z. L. Liao, S. C. Palmateer, S. H. Groves, J. N. Walpole, and L. J. Missaggia, "Low-threshold InGaAs strained-layer quantum-well lasers ($\lambda = 0.98 \mu\text{m}$) with GaInP cladding layers and mass-transported buried heterostructure," *Appl. Phys. Lett.*, vol. 60, pp. 6-8, 1992.
- [11] M. A. Haase, M. J. Hafich, and G. Y. Robinson, "Internal photoemission and energy-band offsets in GaAs-GaInP p-i-n heterojunction photodiodes," *Appl. Phys. Lett.*, vol. 58, pp. 616-618, 1991.
- [12] $\Delta E_C = 198 \text{ meV}$ is reported in D. Biswas, N. Debbar, and P. Bhattacharya, M. Razeghi, M. Defour, and F. Omnes, "Conduction- and valence-band offsets in GaAs/Ga_{0.51}In_{0.49}P single quantum well grown by metalorganic chemical vapor deposition," *Appl. Phys. Lett.*, vol. 56, pp. 833-835, 1990.
- [13] S. Adachi, "GaAs, AlAs, Al_xGa_{1-x}As: Material parameters for use in research and device applications," *J. Appl. Phys.*, vol. 58, pp. R1-R29, 1985.
- [14] J. M. Kuo, Y. K. Chen, M. C. Wu, and M. A. Chin, "InGaAs/GaAs/InGaP multiple quantum well lasers prepared by gas-source molecular beam epitaxy," *Appl. Phys. Lett.*, vol. 9, pp. 2781-2783, 1991.
- [15] Y. K. Chen, M. C. Wu, W. S. Hobson, S. J. Pearton, A. M. Sergent, and M. A. Chin, "High power 980 nm AlGaAs/InGaAs strained quantum well lasers grown by OMVPE," *IEEE Photon. Technol. Lett.*, vol. 3, pp. 409-411, 1991.
- [16] R. J. Fu, C. S. Hong, E. Y. Chan, D. J. Booher, and L. Figueroa, "High-temperature operation of InGaAs strained quantum well lasers," *IEEE Photon. Technol. Lett.*, vol. 3, pp. 308-310, 1991.

- [17] P. S. Zory, A. R. Reisinger, R. G. Waters, L. J. Mawst, C. A. Zmudzinski, M. A. Emanuel, M. E. Givens, and J. J. Coleman, "Anomalous temperature dependence of threshold for thin quantum well AlGaAs diode lasers," *Appl. Phys. Lett.*, vol. 49, pp. 16-18, 1986.
- [18] D. Botez, J. C. Connolly, and D. B. Gilbert, "High-temperature cw and pulsed operation in constricted double-heterostructure AlGaAs diode lasers," *Appl. Phys. Lett.*, vol. 39, pp. 3-6, 1981.
- [19] M. C. Wu, Y. K. Chen, M. Hong, J. P. Mannaerts, M. A. Chin, and A. M. Sergent, "A periodic index separate confinement heterostructure quantum well laser," *Appl. Phys. Lett.*, vol. 59, pp. 1046-1048, 1991.
- [20] Y. K. Chen, M. C. Wu, J. M. Kuo, M. Chin, and A. M. Sergent, "Self-aligned InGaAs/GaAs/InGaP quantum well lasers prepared by gas-source molecular beam epitaxy with two growth steps," *Appl. Phys. Lett.*, vol. 59, pp. 2929-2931, 1991.

Spectral Linewidth of MQW DFB Lasers with Intensity-Modulated TM-Polarized Light Injection

Hiroshi Yasaka, Kazuo Kasaya, Kiyoto Takahata, and Mitsuru Naganuma

Abstract—The spectral linewidth of a multiple-quantum-well (MQW) distributed feedback (DFB) laser is measured when intensity-modulated orthogonally-polarized (transverse magnetic (TM) mode) light is injected into the laser. The spectral linewidth does not change when the modulation frequency is higher than several hundred megahertz and is almost the same as without light injection. However, it broadens when the injected orthogonally polarized light modulation frequency is close to zero. The line shape of the MQW DFB laser's lasing light becomes non-Lorentzian in shape below a modulation frequency of 500 MHz.

INTRODUCTION

CONTROL of the semiconductor laser lasing mode with light injection will be valuable for high-speed all-optical transmission, switching, and computing systems. This is because both the thermal and parasitic effects can be excluded by using this control method. The use of light injection for lasing mode control has been tried for lasing mode frequency and intensity modulation [1]-[5]. In most of these trials, however, the wavelength of the injected light was set much shorter than that of the controlled semiconductor laser. We have demonstrated that intensity-modulated orthogonally polarized light permits the lasing mode of distributed feedback (DFB) lasers to operate at the laser's intrinsic response speed, free from thermal and parasitic effects [6]-[9]. In these cases, the wavelength of the injected light was set almost the same as that of the lasing mode, but with an orthogonal polarization.

Manuscript received February 4, 1992; revised April 9, 1992.

The authors are with the NTT Opto-electronics Laboratories, Koganei-City, Pref. 243-01, Japan.

IEEE Log Number 9201688.

This letter is the first report on the spectral linewidth behavior of an MQW DFB laser injected with intensity-modulated orthogonally polarized light.

EXPERIMENTS AND RESULTS

A 1.55- μm MQW DFB laser with a buried heterostructure (BH) was used in this experiment. The MQW active layer consisted of six InGaAs wells separated by InGaAsP barriers ($\lambda_g = 1.3 \mu\text{m}$). The thicknesses of each well and barrier were 50 and 100 Å, respectively. A corrugation grating was formed with a $\lambda/4$ -shift in the center of the laser cavity. The laser's cavity was 500 μm long and the κL was about 2.4. The facets were coated with an SiN_x antireflection film. Residual facet reflectivity was estimated to be 0.5%. The threshold current and the differential efficiency per facet were 16 mA and 0.1 mW/mA. Single-mode operation was maintained at bias currents of up to 200 mA.

The experimental setup is shown schematically in Fig. 1. Two single-mode distributed Bragg reflector ($\text{DBR}_{1,2}$) lasers were used to generate intensity-modulated light. The wavelengths of these lasers were 1.53 μm . Optical isolators OI's (isolation of more than 60 dB) were inserted in front of the DBR lasers to avoid that the reflected light and output light from the MQW DFB laser couple to the lasers. The light beams passing through the optical isolators were mixed by a half mirror HM and the intensity of the mixed beam was modulated. The modulation frequency of the light was coincident with the optical frequency deviation of the two lasers and was changed by changing the bias current to one of the lasers. The modulation frequency was monitored by monitoring the beat spectrum between the two DBR lasers using spectrum